



Changes of the aridity index in Europe from 1950 to 2019

Zuzana Bešťáková^{1,2} · Filip Strnad¹ · Mijael Rodrigo Vargas Godoy¹ · Ujjwal Singh¹ · Yannis Markonis¹ · Martin Hanel¹ · Petr Máca¹ · Jan Kysely^{1,2}

Received: 19 October 2021 / Accepted: 26 October 2022 / Published online: 29 November 2022
© The Author(s), under exclusive licence to Springer-Verlag GmbH Austria, part of Springer Nature 2022

Abstract

The aridity index, also known as the Budyko index, describes spatiotemporal changes in the hydroclimatic system in the long-term perspective. Defined as the ratio between potential evapotranspiration and precipitation, it can be used to determine wet (humid) and dry (arid) regions. In this study, we evaluated the aridity index estimated in different temporal scales, investigated its spatial patterns, and highlighted the long-term changes in Europe using three gridded data sets (CRU, E-OBS, and ERA5). A significant dry region expansion is evident in all data sets since the late 1980s. The extent of the dry regions has increased in Western, Central, and Eastern Europe, especially at low and medium altitudes. The results show the long-term development of the European hydroclimatic system and which areas have changed from wet to dry.

Keywords Aridity index · Budyko curve · Potential evapotranspiration · Precipitation · Drought · Europe

1 Introduction

Drought affects millions of people worldwide each year (Dai 2011). In particular, it has become increasingly widespread in Europe in the recent decades (Markonis et al. 2021; Moravec et al. 2021) and has been causing more and more problems in various socio-economic sectors like agriculture, water resources, and industry (Naumann et al. 2021). Droughts are expected to be more frequent, severe, and prolonged in the future (Ault 2020; Rakovec et al. 2022). Severe droughts significantly impact on the hydroclimatic system (Wilhite 2000; Keyantash and Dracup 2004; Van Loon 2015), so it is crucial to investigate droughts based on the long-term behavior of the hydroclimatic system and seek solutions and mitigation strategies.

The aridity index describes the long-term functioning of the atmosphere, more specifically, the process of receiving and releasing water from the underlying surface hydrological system. We study the potential flow of water to the atmosphere, assuming that we have an unlimited

water supply (Budyko 1974; Wang and Alimohammadi 2012; Blöschl et al. 2013; Creed et al. 2014). In an arid/dry environment (d), evapotranspiration prevails over precipitation, and vice versa in a humid/wet environment (w).

The aridity index is one of the primary inputs of the Budyko modeling framework (Budyko 1974; Arora 2002; Gerrits et al. 2009; Blöschl et al. 2013; Zhou et al. 2015; Carmona et al. 2016). Budyko (1974) defined the aridity index as the ratio of potential evapotranspiration (defined in Section 2.1) to precipitation (PET/P).

Many authors applied the aridity index to characterize long-term runoff or actual evapotranspiration (Arora 2002; Zheng et al. 2009; Wang and Alimohammadi 2012; Blöschl et al. 2013; Creed et al. 2014). Among them, Arora (2002) used the aridity index to obtain an analytic formula to estimate the change in runoff under annual changes in precipitation and available energy. Long-term actual evapotranspiration can be calculated based on the aridity index according to the Budyko hypothesis, which describes actual evapotranspiration as a function of the aridity index (Zheng et al. 2009). According to the United Nations Environment Programme (Barrow 1992) and other authors (Lioubimtseva et al. 2005; Diaz-Padilla et al. 2011; Spinoni et al. 2015; Huang et al. 2016; Zhao et al. 2019; Myronidis and Nikolaos 2021), the aridity index can also be defined as the ratio P/PET . In this study, the aridity index is defined as PET/P (Arora 2002; Gerrits et al. 2009; Nyman et al. 2014; Zhou et al. 2015; Carmona et al. 2016; Liu et al. 2019).

✉ Zuzana Bešťáková
bestakova@ufa.cas.cz; bestakova@fzp.czu.cz

¹ Faculty of Environmental Sciences, Czech University of Life Sciences, Prague, Czech Republic

² Institute of Atmospheric Physics, Czech Academy of Sciences, Prague, Czech Republic

Studies reporting aridity change on a global scale observed an increase in aridity index (AI) in Europe (Gao and Giorgi 2008; Spinoni et al. 2015; Huang et al. 2016). However, these analyses are performed at a very coarse scale, prohibiting the detection of any regional signal. Regional-scale studies show similar results, but most of them focus on small areas in southern or southeastern Europe (Paltineanu et al. 2007; Gao and Giorgi 2008; Salvati et al. 2013; Pravalie and Bandoc 2015; Spinoni et al. 2015; Huang et al. 2016; Cheval et al. 2017; Myronidis and Nikolaos 2021). There is general agreement on the development of dry areas among authors who study AI-based climate change. However, no study has dealt with the long-term development of AI in Central, Eastern and Western Europe. Other studies focus on different areas or global scales and do not provide regional details. We did not find any study dealing with Central (defined here as 45–55° latitude and 6–24° longitude), Eastern (east of 24° longitude), or Western Europe (west of 6° longitude) specifically.

2 Data and methods

2.1 Potential evapotranspiration

Potential evapotranspiration is defined as the amount of water transpired by a short crop layer of uniform height continuously shading the soil and having sufficient water in the soil (Peng et al. 2017). In contrast, reference evapotranspiration is crop-specific and used at the local scale, especially by agronomists (Allan et al. 1998; Oudin et al. 2005; Seiller and Anctil 2016; Peng et al. 2017; Kohli et al. 2020; Xiang et al. 2020). Potential evapotranspiration can be converted into reference evapotranspiration when multiplying it by the appropriate crop coefficient, which provides an estimate of crop water use. If land use data are unavailable (or not considered), this coefficient cannot be estimated (Seiller and Anctil 2016). Since we do not have land-use data available and focus on spatiotemporal changes in the hydroclimatic system in the long-term perspective, potential evapotranspiration is used to calculate the aridity index. The difference between the potential evapotranspiration and the reference crop evapotranspiration is discussed in detail by (Xiang et al. 2020).

In many studies, potential evapotranspiration and reference evapotranspiration are confused, and in such studies, they are also compared to each other (Winter et al. 1995; Xu and Singh 2000; Tabari 2010; Tegos et al. 2015; Poyen et al. 2016; Seiller and Anctil 2016). The problem was pointed out by Xiang et al. (2020). Xu and Singh (2000) and Xiang et al. (2020) divided the methods for calculating

potential and reference evapotranspiration into four groups: mass transfer type, temperature-based type, radiation type, and combination type.

In general, the most often used equations are of the temperature-based type. The most widely used method of this type is the Thornthwaite equation, as it is simple and requires only temperature for calculation (Pereira and Pruitt 2004; Bautista et al. 2009; Chang et al. 2019), but has been found to underestimate reference evapotranspiration (Pereira and Pruitt 2004; Sentelhas et al. 2010; Lakatos et al. 2020; Xiang et al. 2020).

The radiation type equations can be viewed as simplified forms of the Penman equation (Gardelin and Lindstrom 1997; Xiang et al. 2020). Among the widely used radiation-based methods is the Turc equation, which shows good results in different studies, but its calculation requires a large number of variables (Xu et al. 2013; Xiang et al. 2020) that are often unavailable.

The combined type includes energy balance and aerodynamic aspects, with the velocity term and vapor pressure being its two basic terms. Penman and Monteith are the basic equations for the combined type, which were then linked (Penman-Monteith formula) and recommended by FAO as a standardized method (Xiang et al. 2020). However, it leads to better estimates only if the input variables are well measured or estimated (they are sensitive to the imprecision of the data (Weiland et al. 2012; Seiller and Anctil 2016)). Another problem is that the Penman-Monteith formula is an equation for calculating reference crop evapotranspiration and should not be used for potential evapotranspiration (Xiang et al. 2020). Also, Weiland et al. (2012) found better model performance using the simplest formulas versus the combination ones, thereby reducing the number of data-intensive input variables. For these reasons, we decided to use the Oudin formula to calculate potential evapotranspiration, which is defined as:

$$PET = \frac{0.408R_e(TG + 5)}{100}, \text{ if } TG + 5 > 0$$

$$PET = 0 \text{ otherwise} \quad (1)$$

where PET [$mm \cdot day^{-1}$] is potential evapotranspiration, R_e [$MJ \cdot m^{-2} \cdot day^{-1}$] is the solar radiation (this is top-of-atmosphere radiation, calculated only based on the time of year and geographical location—the influence of the atmosphere is not considered), and TG [$^{\circ}C$] is mean daily air temperature (Oudin et al. 2005).

We chose the calculation of potential evapotranspiration according to the Oudin formula (which also belongs to the radiation type equations) because it provides the most adequate PET input to rainfall-runoff models. Oudin et al. (2005) tried to identify the most relevant approach to calculating PET and concluded that formulas based only on temperature and radiation provide the best results. Lang

et al. (2017) also pointed to better results of such methods and Tegos et al. (2015) reported that the Oudin formula shows relatively good results in Europe. Another advantage is data simplicity, as the coverage of meteorological stations is not always sufficient, so it is not possible to use formulas with large data requirements. In addition unlike the extended Thornthwaite formula, the Oudin formula is applicable for average daily temperatures already from -5°C (Oudin et al. 2005).

2.2 Aridity index

In line with the original Budyko's concept, we use the following definition of the aridity index:

$$AI_T = \frac{PET_T}{P_T}, \quad (2)$$

where $AI_T[-]$ is the dimensionless aridity index, $PET_T [mm]$ is potential evapotranspiration, and $P_T [mm]$ is precipitation aggregated over interval T (Gerrits et al. 2009; Wang and Alimohammadi 2012; Creed et al. 2014; Zhou et al. 2015; Carmona et al. 2016).

2.3 Transitions, states, patterns

We study transitions between wet (w) and dry (d) hydroclimatic systems. Transitions for different aggregations ($T = 1, 10, 20, 30$ years) are defined based on the magnitude of the $AI_T(t-1)$ value in the previous period $t-1$ and the $AI_T(t)$ value in the current period t .

If the value of AI in the previous period is less than one and in the current period greater than one (transition wd), a wet grid cell shifts into the dry state in the successive periods. If the value of AI in the previous period is greater than one and in the current period less than one (transition dw), the dry state changes into the wet state. If the AI value in the previous and current period is less than one (pattern ww), a wet state is attributed to both periods for a given grid cell. If the value of AI in the previous and current periods is greater than one (pattern dd), a dry state is attributed to the given grid cell in both periods. When determining the relative frequencies of transitions, states, and patterns for a larger area, we weighted them by the area of the grid cells at a specific latitude.

2.4 Gridded data sets used for the analyses

This section presents the three gridded data sets applied in this work: Climatic Research Unit (CRU) TS version 4.04, E-OBS version 22.0e, and the European Centre for Medium-range Weather Forecasts (ECMWF) ERA5 reanalysis. The whole study deals with hydrological years starting on November 1 and ending on October 31; this

definition is set so that there is no significant year-to-year transfer of precipitation in the snow cover.

E-OBS has a resolution of $0.25^{\circ} \times 0.25^{\circ}$ and is available for 1920–2020. The daily precipitation and average daily temperature values come from the E-OBS 22.0e data set released in May 2020 (Cornes et al. 2018). The annual precipitation totals were calculated based on monthly values, and potential evapotranspiration was based on daily temperature values according to the Oudin formula (Oudin et al. 2005; Sarbu and Sebarchievici 2017; Wald 2018). Studies analyzing E-OBS (Hofstra et al. 2009; Herrera et al. 2012; Skok et al. 2016; Navarro et al. 2019) have reservations about the density of the station network or their inhomogeneous coverage. The highest density of stations is in Northern Europe, England, Central Europe, and northern Italy, while the network of stations is sparsest in Southern and Eastern Europe (Cornes et al. 2018; Navarro et al. 2019). The accuracy of E-OBS strongly depends on the density of the station network, and sparsely covered areas have less accurate data. E-OBS was evaluated as better than ERA5 in regions with dense data, while in areas with sparse data both data sets are at the same level (Bandhauer et al. 2022).

CRU is a data set with a resolution of $0.5^{\circ} \times 0.5^{\circ}$, produced at the University of East Anglia and available for 1901–2019. It is a monthly gridded observational data set, spatially interpolated. The interpolation is based on angular-distance weighting. Available PET in this data set is estimated using the Penman-Monteith formula (Harris et al. 2020), which includes the mean, maximum and minimum temperature, vapor pressure, cloud cover, and wind speed (Harris et al. 2014). The Penman-Monteith formula is in fact a reference crop evapotranspiration (mass transfer type; (Xiang et al. 2020)), so it was not used in our study; the Oudin formula was used instead to calculate the potential evapotranspiration.

ERA5 is the fifth generation of ECMWF reanalysis for the global climate and weather. The ERA5 is a grid data set with a resolution of $0.25^{\circ} \times 0.25^{\circ}$, available for 1950–2020. The data is obtained from the Climate Data Store entries (Hersbach et al. 2018; Bell et al. 2020) and applies the Hargreaves-Samani formula for potential evapotranspiration (Hargreaves and Samani 1985). The formula uses the average, maximum, and minimum temperature, evaporation equivalent, and empirical coefficient for the calculation (Rolle et al. 2021). The Hargreaves-Samani formula is also a reference crop evapotranspiration (temperature-based type; Xiang et al. (2020)), and its implementation in ERA5 contains a code error (transpiration is zero in areas without vegetation—coastal and dry regions). The Oudin formula was used in this study also for ERA5.

The primary parameters determined by the different grid models were used to calculate Oudin-type PET and then

compared to the PET calculated by ERA5 and CRU teams (Fig. 1). There is a significant underestimation of available PET in coastal areas in ERA5 and a slight underestimation in the UK and the Po Valley in CRU. On the contrary, the overestimation in ERA5 and CRU is evident mainly in Southern Europe (south of 45° latitude), especially in the Iberian Peninsula.

The spatial resolution of $0.5^\circ \times 0.5^\circ$ of all data sets was used for computation and analysis (the raster package (Hijmans 2021) in R environment was used for aggregation in E-OBS and ERA5). Most of Europe (13° W – 30° E longitude, 30°–70° N latitude) is studied here. Furthermore, the stats package in R environment (Wickham 2016; R Core Team 2021) is used to create empirical quantile-based distribution functions and construct the probability density.

3 Results

3.1 Basic properties

The increase in the mean AI over the whole period is shown in Fig. 2. For two out of the three data sets, the mean value decreased from 1960 to 1969 and considerably increased thereafter. ERA5 increasing trend lags behind the other two starting only at the end of the 1970s.

The mean and standard deviation of AI in Europe for 10-year aggregations for each transition and pattern are shown in Table 1. A decrease in the mean of AI values was found in the *dd* pattern during 1960–1979 and a subsequent sharp increase in the 1980–1989 period in all three data sets (Table 1). A decrease and subsequent gradual increase

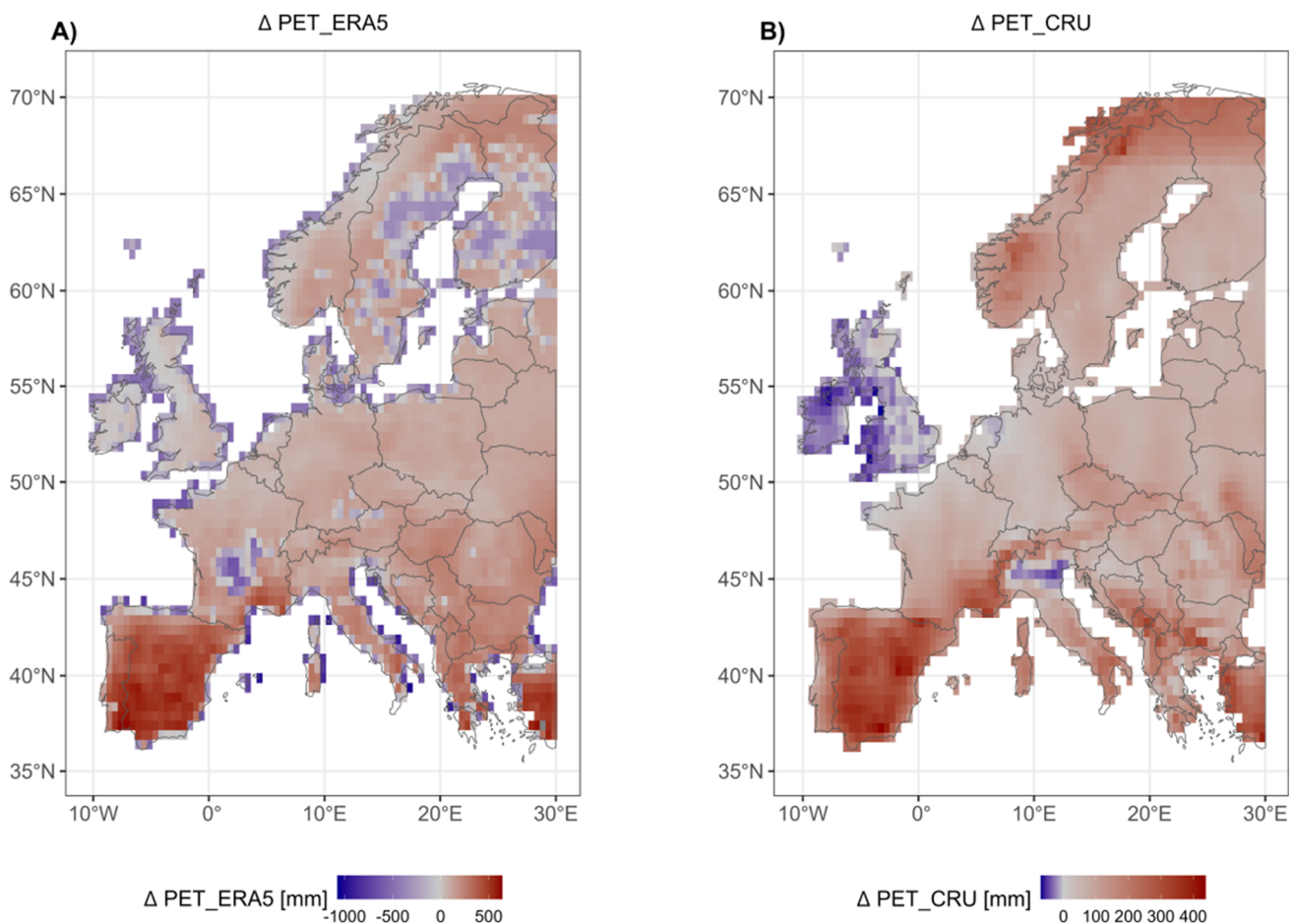
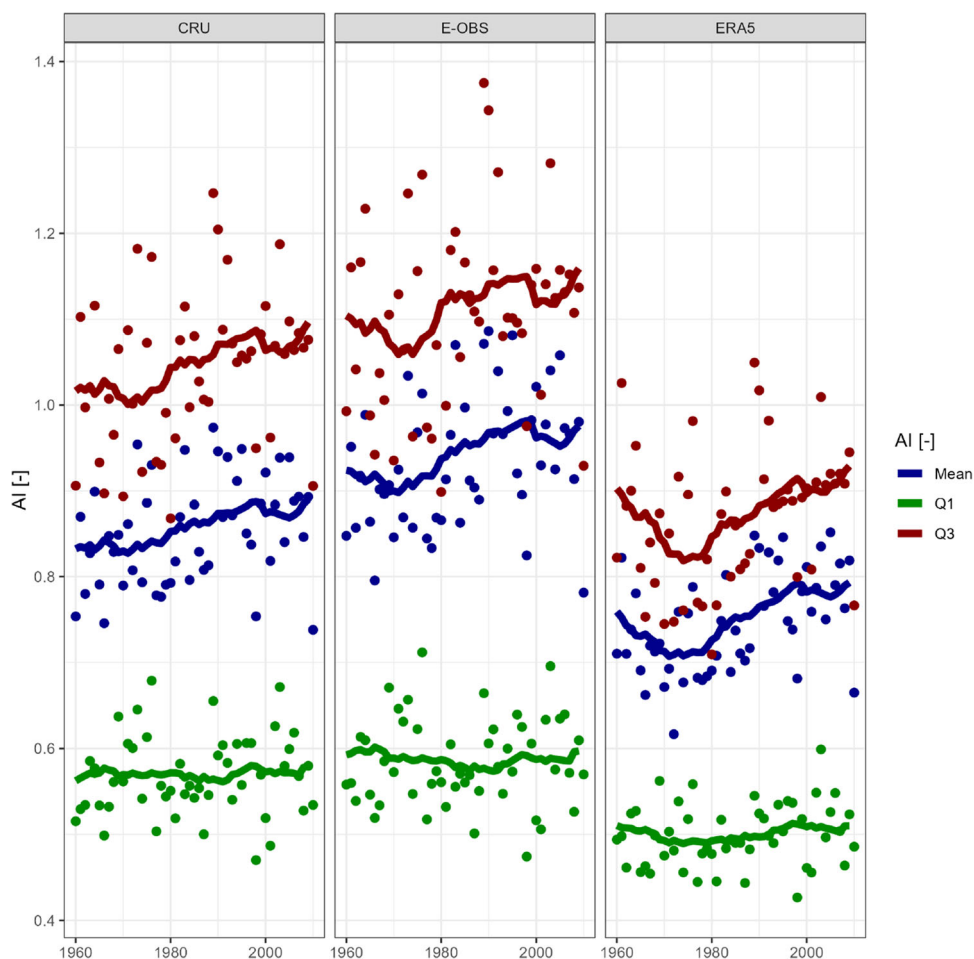


Fig. 1 Differences between mean annual values of A) PET calculated by ERA5 team (Hargreaves-Samani formula) and PET according to the Oudin formula (Δ PET_ERA5, left), B) PET calculated by CRU team

(Penman-Monteith formula) and PET according to the Oudin formula (Δ PET_CRU, right), for 1950–2019

Fig. 2 20-year moving averages of annual mean, the lower quartile (Q1) and upper quartile (Q3) of AI values (solid lines) for all data sets for 1950–2019. Points show values in individual years; the lower and upper quartiles are estimated from the distribution across all grid boxes in the analysed area (Europe)



were also partly found in the dw and wd transitions in all data sets. Standard deviation increased during the 1990–1999 period for the pattern dd in E-OBS and ERA5, and the highest value for CRU was found in the 1980–1989 period. For the ww pattern, the changes in mean values are negligible, and only in ERA5 there is a slight decrease during the 1960–1989 period.

Empirical quantile-based distribution functions for all three data sets are compared in Fig. 3A. There is a considerable underestimation of AI values in ERA5 compared to the other two data sets. Figure 3B shows the different shapes of the probability density functions for each data set. If the AI is around 1, there is a transition from wet to dry and vice versa. The density is plotted on the y -axis.

3.2 Transitions between wet and dry regions

The average AI values (Fig. 4) classified similar proportions of wet and dry regions for the whole period investigated here in CRU and E-OBS, while ERA5 shows wet environments over most of the study area instead. In the CRU and E-

OBS data wet regions occur all over Northern Europe (north of 55° latitude) and the UK, while dry regions in Southern Europe, the Pannonian Basin, Moldova, Ukraine, Poland, Czechia, the northeastern part of Germany, and the French Lowlands. In contrast, ERA5 shows wet conditions in the North-German Lowland, the Wielkopolska Lowland, Belarus and northern Ukraine. These additional wet conditions in ERA5 could be caused by the overestimation of precipitation (see Section 4).

Western, Central, and Eastern Europe form a transition strip (white color). The term “transition strip” is defined here as the central latitude strip of Europe (between 45° – 55° latitude, and 5° – 30° longitude). The most significant changes in the development of dry areas take place within this region.

We identified regions with the largest differences between consecutive mean AI values for 20-year periods (Fig. 5). During 1980–1999, there was a substantial increase in AI in Southern Europe, while in 2000–2019, drying took place mainly in the transition strip. Although the data sets share an overall similar signal for dry region development,

Table 1 Mean and standard deviation of mean values of AI for each transition (*dd*, *ww*) and pattern (*dw*, *wd*) in individual grid boxes for 10-year periods

10-year	Period	Mean_dd	sd_dd	Mean_dw	sd_dw	Mean_wd	sd_wd	Mean_ww	sd_ww
CRU	1950–1959	1.42	0.36	1.03	0.14	0.98	0.14	0.61	0.22
	1960–1969	1.36	0.33	0.94	0.13	0.95	0.12	0.60	0.23
	1970–1979	1.35	0.32	0.96	0.12	0.97	0.13	0.61	0.23
	1980–1989	1.48	0.43	1.01	0.11	0.98	0.15	0.61	0.23
	1990–1999	1.42	0.41	0.97	0.14	0.98	0.14	0.61	0.24
	2000–2009	1.44	0.40	0.98	0.13	0.97	0.12	0.61	0.23
	2010–2019	1.43	0.40	1.01	0.14	1.01	0.15	0.61	0.24
E-OBS	1950–1959	1.59	0.52	1.00	0.16	1.00	0.15	0.63	0.21
	1960–1969	1.48	0.49	0.95	0.15	0.96	0.13	0.61	0.22
	1970–1979	1.49	0.45	0.95	0.14	0.97	0.15	0.62	0.22
	1980–1989	1.64	0.57	1.01	0.12	0.99	0.16	0.61	0.22
	1990–1999	1.60	0.60	0.98	0.16	0.99	0.16	0.61	0.22
	2000–2009	1.60	0.58	0.98	0.17	0.97	0.16	0.61	0.22
	2010–2019	1.54	0.54	1.01	0.16	1.01	0.16	0.62	0.23
ERA5	1950–1959	1.51	0.46	0.98	0.17	0.98	0.16	0.60	0.22
	1960–1969	1.40	0.44	0.91	0.16	0.94	0.14	0.57	0.20
	1970–1979	1.37	0.33	0.95	0.17	0.97	0.17	0.57	0.20
	1980–1989	1.54	0.44	0.99	0.13	0.95	0.18	0.56	0.20
	1990–1999	1.51	0.47	0.96	0.16	0.98	0.16	0.58	0.21
	2000–2009	1.55	0.44	1.00	0.17	0.99	0.16	0.59	0.21
	2010–2019	1.49	0.47	0.97	0.15	0.97	0.15	0.58	0.21

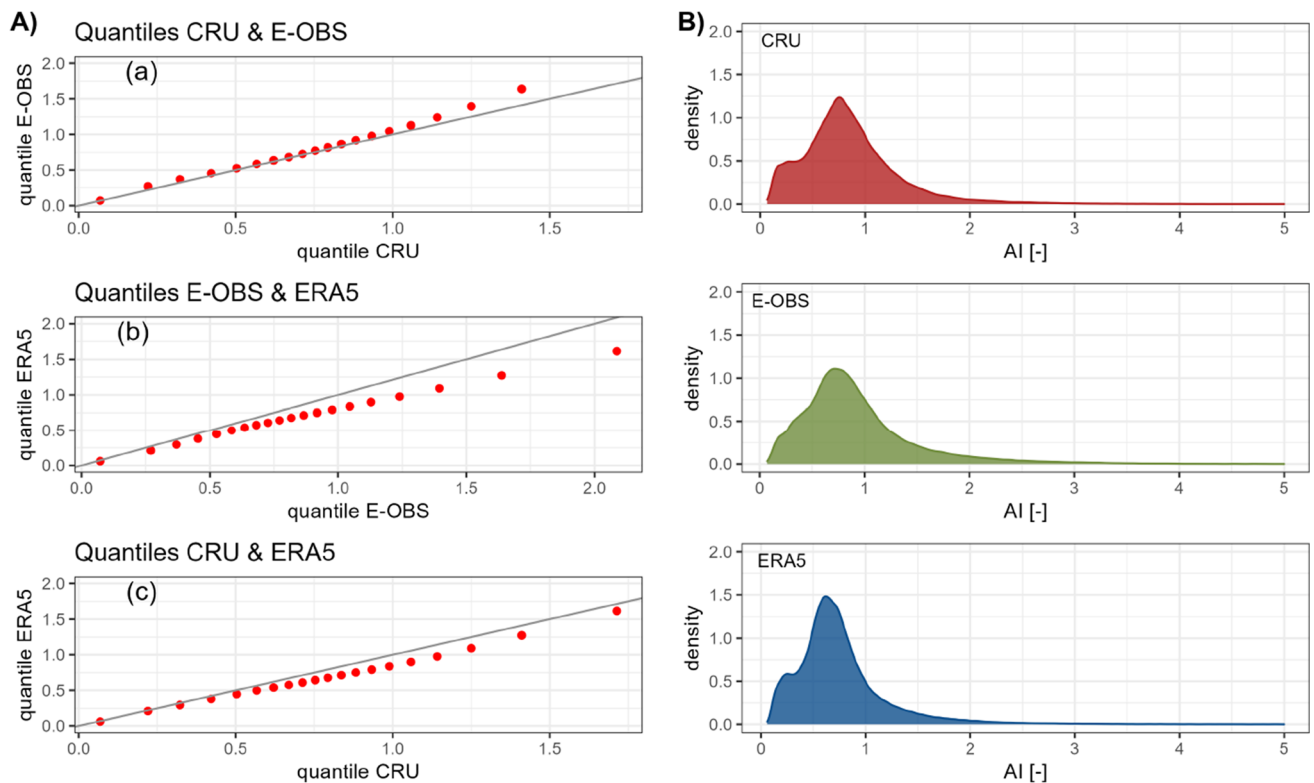
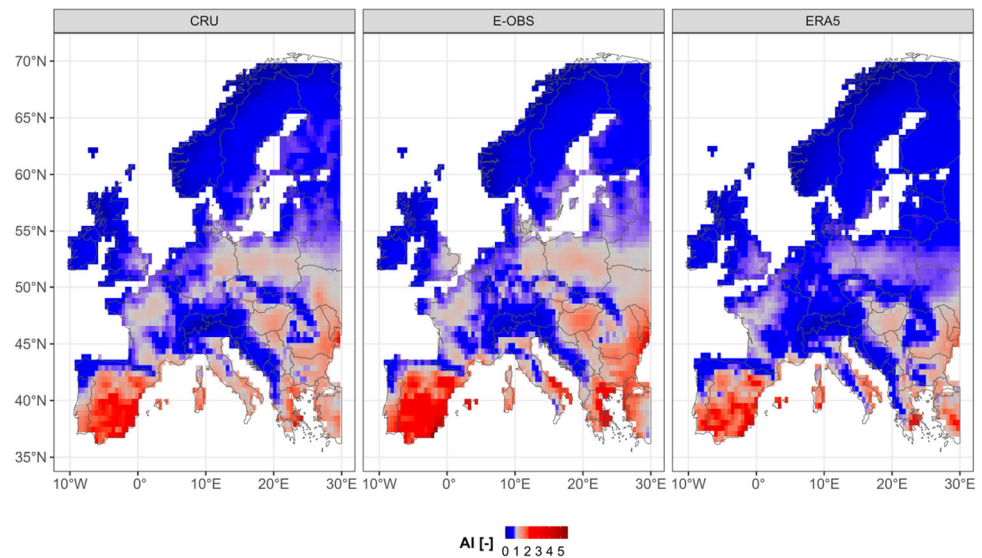
**Fig. 3** A Quantile-quantile plots of annual AI values for 1950–2019: (a) CRU and E-OBS, (b) E-OBS and ERA5, (c) CRU and ERA5. B Probability density of annual AI values for 1950–2019. The x-axis shows the AI values and the y-axis the density

Fig. 4 Average AI values for the whole period (1950–2019) for each grid cell



the location of the hotspots differs; CRU in Western Europe, E–OBS in Central and Western Europe, and ERA5 in Eastern Europe (Figs. 5 and 7).

The 10-year moving average of annual AI values were compared with those of the previous 10-year periods. States (d , w), transitions (wd , dw), and patterns (ww , dd) were assigned to these AI values (Fig. 6). According to the three data sets' median, the probability of occurrence of dry regions has increased by approximately 7% over the last 50 years (Fig. 6). The most intense increase has been observed since the late 1980s (approximately 8%). The above is also reflected in the behavior of the dd and ww patterns. Over the last 50 years, there has been an increase in the dd pattern by approximately 3% and a decrease in ww by approximately 1%. The ww pattern was most frequent in the mid-1980s, followed by a considerable decrease, i.e., an increase in dry regions. The dw transitions decreased from 1970s until mid-1980s, then increased considerably from the mid to late 1980s. The incidence of the wd transition increased considerably from the mid-1980s to the beginning of the twenty-first century and then grew slightly. The dw transition has a declining trend throughout the whole period, and the wd transition has an increasing trend. The three data sets found similar trends in transitions, patterns, and states throughout the period. The median trend (black) almost overlaps with CRU.

After plotting the transitions and patterns (wd , dw , ww , dd) for 20-year periods, we found only negligible changes towards drying in Northern Europe and the southeast UK (Fig. 7).

In Southern Europe, there is a gradual expansion of the dry region. In all data sets, the east coast of the Adriatic Sea is included within a wet region, although it is a dry

area in fact due to unique geomorphologic features of the Dinaric Mountains with subterranean rivers and streams. The relatively high precipitation amounts may be related to windward effects on the slopes of the Dinaric Mountains when Mediterranean cyclones influence the region.

A large area of Eastern Europe belongs to the dry area in the CRU and E–OBS, while in ERA5 a significant part of Eastern Europe belongs to the wet area. The spread of drought in Eastern Europe has taken place over the last two decades in CRU and E–OBS, especially in western Ukraine.

Western Europe has been drying up mainly in the French Lowlands; Eastern Europe mainly in northern Ukraine and southern Belarus; and Central Europe from the east, especially in the Pannonian Basin, the Wielkopolska Lowlands, eastern part of the North-German Lowlands, and Czechia (according to CRU and E–OBS).

Southern Europe, the Pannonian Basin, Moldova, Ukraine, Poland, Czechia, the northeastern part of Germany, and the French Lowlands are evaluated as dry areas of Europe according to CRU and E–OBS data sets.

No development of dry regions has taken place at high altitudes. The high mountains remain entirely in the wet region (Figs. 4 and 7), even though drying occurs in these parts of Europe (Fig. 5).

4 Discussion

Our study supports previous results concerning development of aridity in Europe and detects these changes, especially in the central latitude strip of Europe (between 45° and 55° latitude).

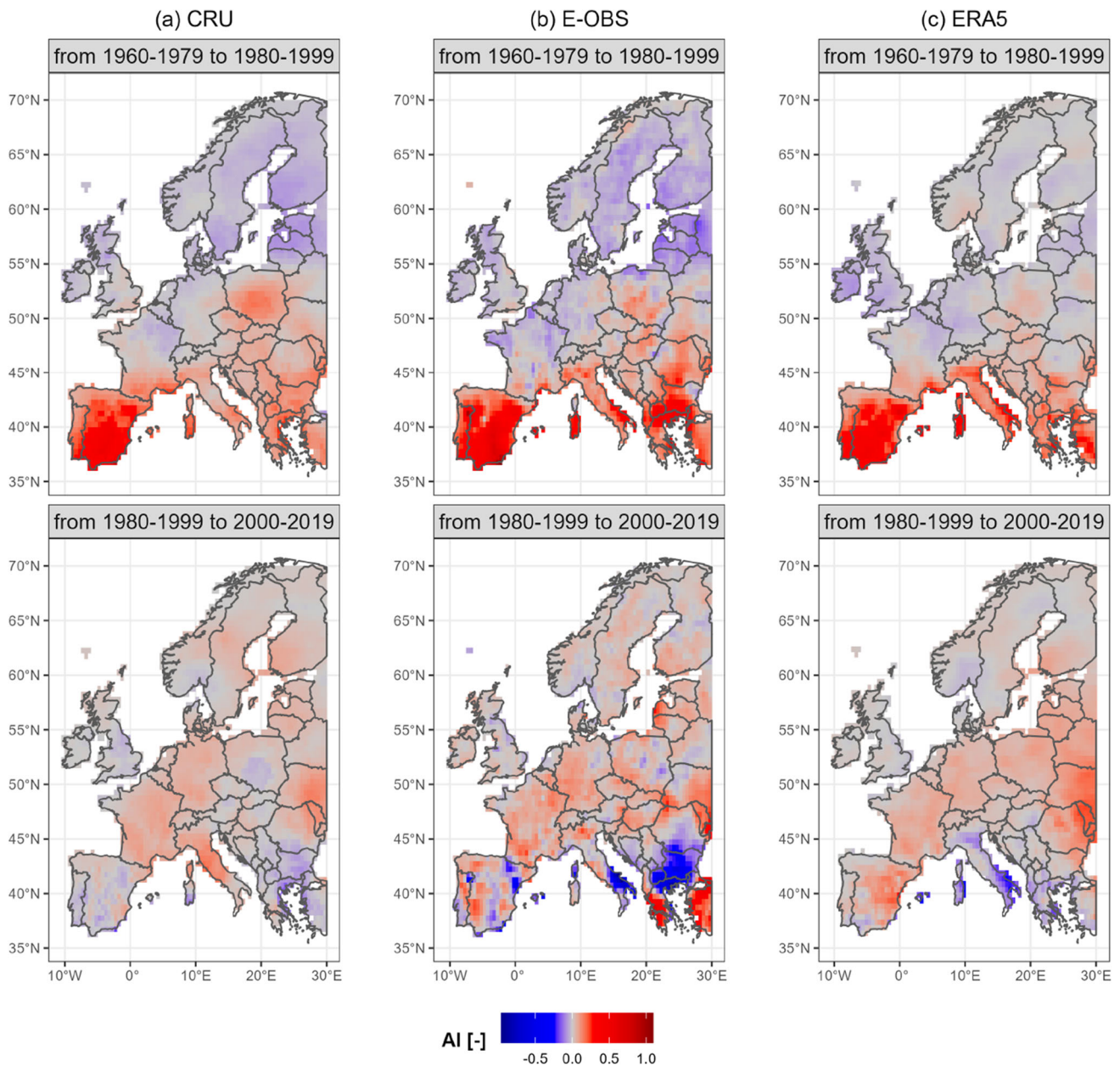


Fig. 5 Differences in mean AI values for the three data sets for consecutive 20-year periods from 1960 to 2019

4.1 Comparison of data sets

The study has identified specific differences between the three data sets related to the different methods for creating them.

Most studies that evaluated precipitation in E-OBS report underestimations in the data (Hofstra et al. 2009; Fibbi et al. 2016; Nechita et al. 2019; Bandhauer et al. 2022). Despite this Nechita et al. (2019) recommend E-OBS for the needs of the current climate data set. According to Laiti et al. (2018), E-OBS shows lower performance in

the Alps compared to ADIGE (regional precipitation and temperature data set (Laiti et al. 2018)) and APGD (the Alpine Precipitation Grid Data set (Isotta et al. 2015)), especially in small river catchments.

Our results are consistent with van der Schrier et al. (2013), who compared CRU and E-OBS and concluded that CRU generally has higher temperature values than E-OBS, which is reflected in our study as higher AI values.

Quite few studies compared observational based data set (E-OBS) and reanalysis data set (ERA5) (Bandhauer et al. 2022; Hassler and Lauer 2021; Velikou et al. 2022).

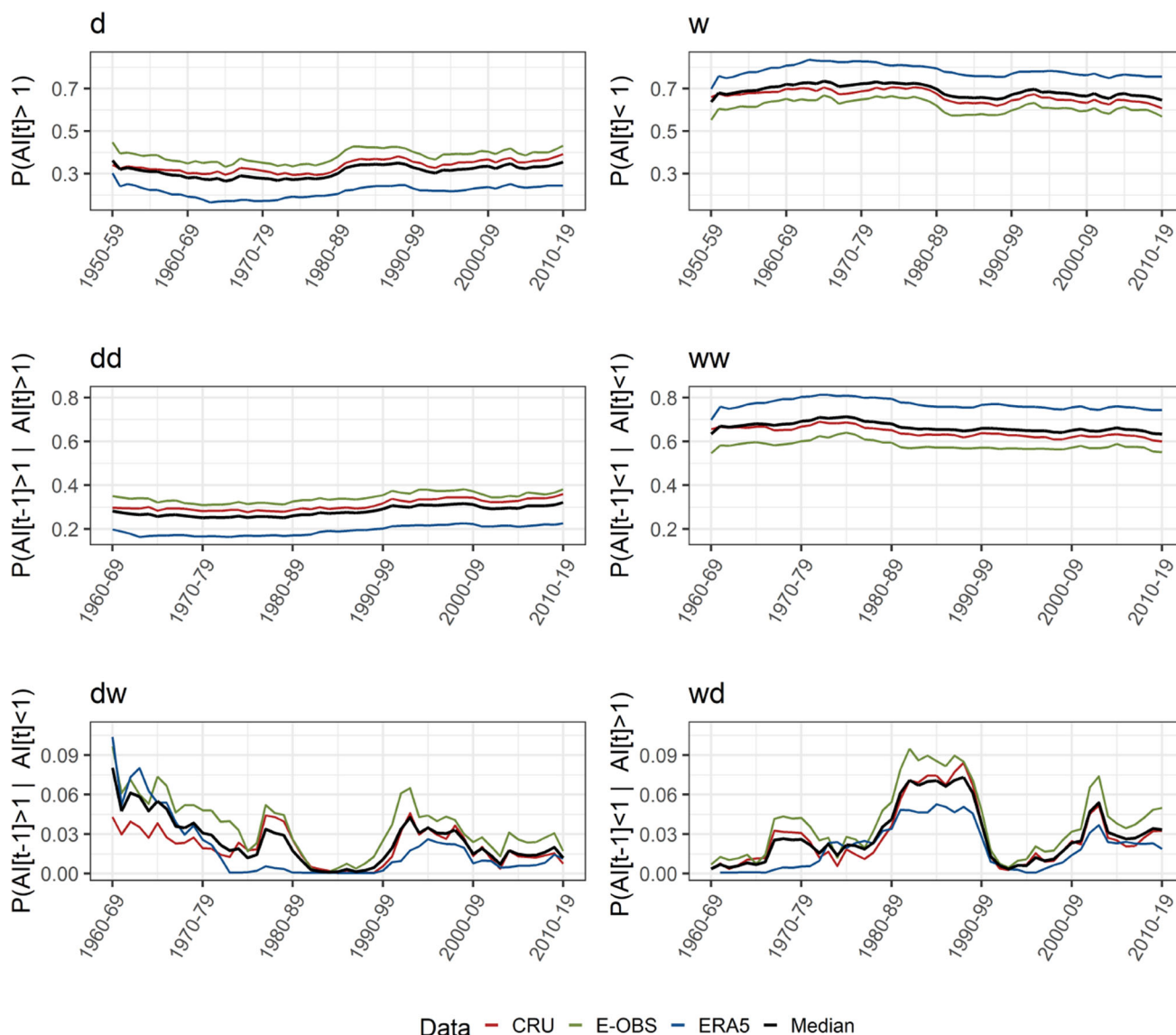


Fig. 6 10-year moving relative frequencies of states (*d*, *w*), patterns (*dd*, *ww*) and transitions (*dw*, *wd*) for 10-year moving periods per unit area for CRU, E–OBS and ERA5. The black line shows the median of all three data sets

Velikou et al. (2022) found underestimated temperatures in ERA5 compared to E–OBS mainly in areas with complex topography, especially in the Alps and the Mediterranean. Bandhauer et al. (2022) and Hassler and Lauer (2021) compared precipitation in E–OBS and ERA5 and concluded that ERA5 overestimated it in Europe (mainly in summer) due to far too many wet days. This is further supported by our results which show considerably wetter conditions in ERA5. We found a substantial difference focused in the area stretching from Central to Eastern Europe.

Bandhauer et al. (2022) emphasized that the underestimation of precipitation in E–OBS is substantially smaller than the overestimation in ERA5. Nevertheless they deemed

both E–OBS and ERA5 as useful data sets for Central and Northern Europe.

Some authors use CRU as a reference (Tapiador and Sanchez 2008; Sanchez et al. 2009) and highlight its advantages: higher spatial resolution than other data sets of similar temporal extent, longer temporal coverage than other products of similar spatial resolution, encompassing a more extensive suite of surface climate variables than available elsewhere, and the construction method ensuring that strict temporal fidelity is maintained (Zvervaev 2004). On the contrary, some studies express reservations—especially about the density of the network of stations or their inhomogeneous coverage (Samani 2000; Zvervaev and

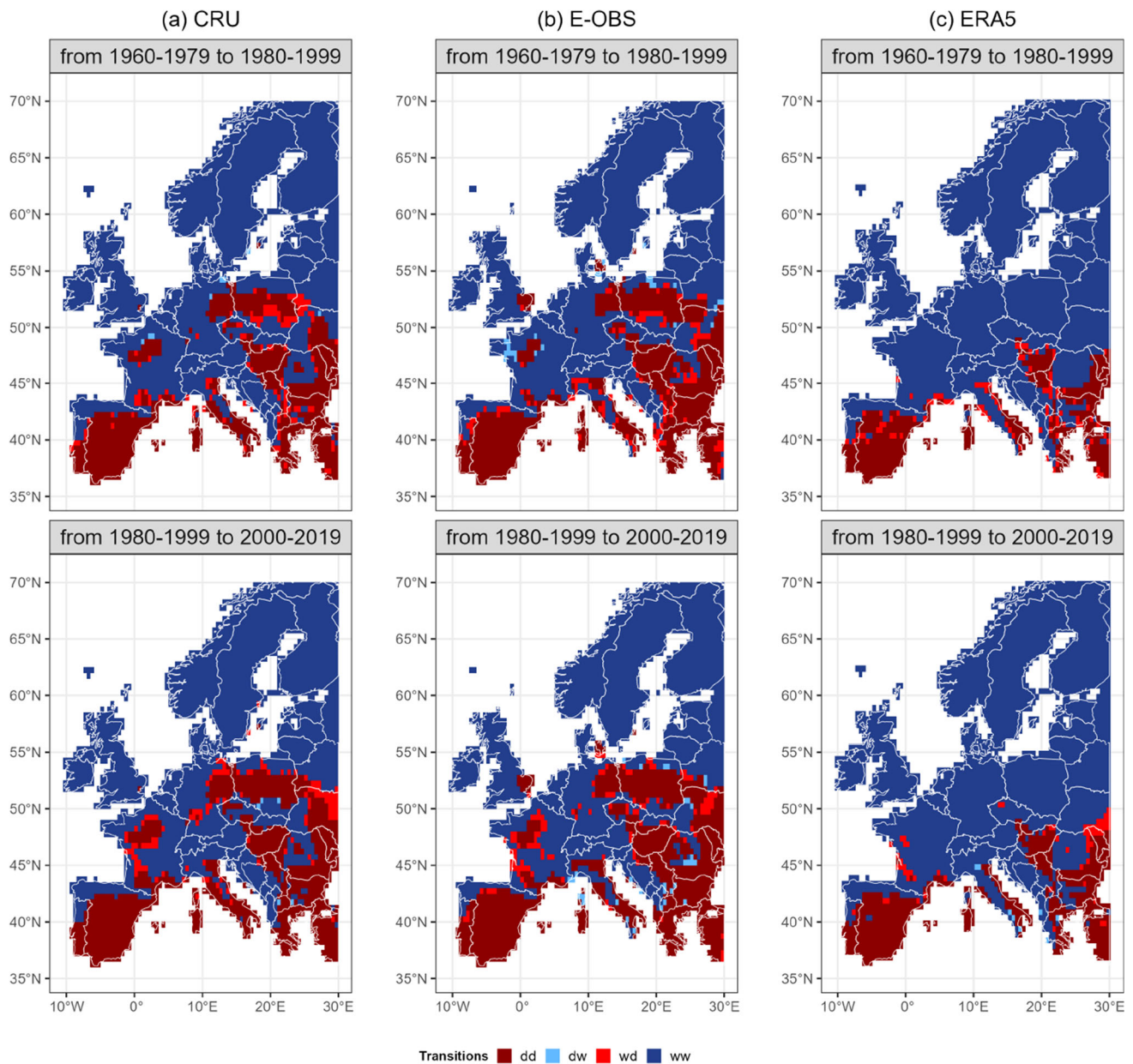


Fig. 7 Transitions (dw , wd), and patterns (dd , ww) for 20-year periods from 1960 to 2019 for the three data sets

Gulev 2009; Tegos et al. 2015; Duan et al. 2019). We do not consider the density of the network of stations to be a problem since the greatest development of drought has taken place in the central latitude strip, and the density of the network is sufficient in this area.

4.2 Temporal development of AI

According to our study, the aridity intensified mainly in the 1950s and from the mid-1980s onward. Unlike existing aridity studies, the results presented herein include the long-term perspective of assessing AI over Europe.

Our results are aligned with those reported by Huang et al. (2016) and Hanel et al. (2018) who identified extreme drought throughout Europe in the early 1950s, the ensuing decline or stagnation, and the renewed considerable increase in dry areas since the 1980s. Nechita et al. (2019) used the CRU, E-OBS, and ROCADA (Birsan and Dumitrescu 2014) data sets to study the Southern Carpathians over 1961–2013. They found wetter climate in the mid-1980s and an increase in extreme temperatures since 1986, manifested as an increase in wd and dd transitions and a decrease in dw and ww transitions in our results. Pan et al. (2021) examined the effect of increasing potential evapotranspiration and

decreasing precipitation on dry regions on the global scale over 1901–2017, and found a global increase in dry areas. Potential evapotranspiration has an increasing trend and weakens the role of precipitation. According to their study, the turning point when potential evapotranspiration exceeded precipitation on a global scale occurred in 1966.

The aridity developed fastest, especially in the period 2000–2019, in the central latitude strip of Europe, namely in northern Ukraine and southern Belarus area, Hungary, Wielkopolska Lowlands, Czechia, North-German Lowlands, and French Lowlands.

Most AI-based drought studies mainly focus on Southern Europe (Gao and Giorgi 2008; Salvati et al. 2013; Spinoni et al. 2015; Huang et al. 2016; Cheval et al. 2017; Myronidis and Nikolaos 2021), in which they report an increase in AI similarly to our study—dry areas are expanding, especially in the Balkan Peninsula and Italy, while drought is deepening in the Iberian Peninsula. Paltineanu et al. (2007) and Pravalie and Bandoc (2015) noticed drought development in Romania and similar results are manifested in our study; most of Romania belongs to the dry area and only the Carpathian region is included in the wet area. Moreover, we observe a more pronounced drought in the Pannonian Basin compared to Romania; a sharp increase in potential evapotranspiration in the Pannonian Basin, especially in its western part at low altitudes, was reported by Lakatos et al. (2020).

Pan et al. (2021) analyzed some areas of Romania as wet catchments, in contrast to our results. This discrepancy may be related to different type of averaging (across catchments vs. grids), a different range of borders between wet and dry catchments in inversely defined AI or a different version of CRU.

AI-based drought studies do not directly address other parts of Europe. We, on the other hand, examined the whole of Europe. No significant changes towards drying were found in Northern Europe. In Southern Europe, there is a gradual variable expansion of the dry region; the largest increase in AI was found during 1980–1999. The most significant changes in the development of dry areas occurred in the transition strip around 50° latitude, and the largest increase in AI was observed there during the period 2000–2019.

Over the past 50 years, the probability of occurrence of dry areas has increased by approximately 7% for the study area. The most intensive increase was observed from the end of the 1980s. The following areas in Europe are classified as dry: Southern Europe, the Pannonian Basin, Moldova, Ukraine, Poland, Czechia, the northeastern part of Germany, and the French Lowlands.

Concerning future scenarios, Gao and Giorgi (2008) estimated further development and an increase in the severity of drought to the north in the dry regions, especially in the central and southern parts of the Iberian, Balkan and Apennine Peninsulas, and on the main islands (Corsica, Sardinia, and Sicily), and then in the Pannonian Basin and Romania. Cheval et al. (2017) reported that the significant relocations to the dry area would occur in southeastern Italy, near the Black Sea, in the eastern part of the Balkan Peninsula, and in the Pannonian Basin. In all of these areas, we find an increase in AI. Furthermore, we observed a significant increase in drought especially in Central Europe, which has not been highlighted as a hot spot in the above-cited studies.

4.3 Drought linked with atmospheric circulation

Physical mechanisms affecting long-term changes in the hydro-climatic system and drought development include atmospheric circulation (e.g. Lhotka et al. (2020)). The dominant mode of climate variability in Europe, especially in the cold half-year, is the North Atlantic Oscillation (NAO). Changes in the intensity of the NAO and the location of its centers of action were reported by many authors (e.g. Kucerova et al. (2017)) and influenced temperature and precipitation trends in Europe over the past decades. They are also related to the shift of storm tracks to the north (Sfica et al. 2021) or northwest (Kucerova et al. 2017) which results in positive atmospheric pressure anomalies over Central Europe (Tomczyk et al. 2019), decrease of cloud cover and development of inland drought (Sfica et al. 2021). Kucerova et al. (2017), Lhotka et al. (2020), and Rehor et al. (2021) reported an increase in anticyclonic circulation types in Central and Eastern Europe, which supports the increase in AI taking place in the central latitude strip. The frequency changes between cyclonic/anticyclonic circulation types as well as between types associated with warm/cold advection and deficit/excess of precipitation are particularly important for droughts and heatwaves in warm half-year, and Lhotka et al. (2020) showed that circulation changes contributed to an increase in drought characteristics over Central Europe since the 1950s. It remains open and subject to follow-up investigation on whether similar changes also played a role in drying trends in other parts of Europe.

Huguenin et al. (2020) linked the record-breaking heatwaves and water shortages in recent years in Central Europe to anthropogenic warming and a weaker jet stream, which allowed the quasi-stationary and high-pressure system to persist for many days. As heatwaves are coupled to soil moisture conditions, these changes (including the

persistence of circulation patterns) will likely influence drought characteristics.

5 Conclusion

Our study examined dry and wet regions in Europe based on the aridity index in space and time over 1950–2019. The main goal was to identify regions where a shift from wet to dry conditions occurred, the period of increased transitions to dry regions, and to compare three widely used continental data sets (CRU, E-OBS, ERA5).

We chose the Oudin formula to calculate potential evapotranspiration for all data sets, because it is the most adequate PET input to rainfall-runoff models. The pronounced change from wet to dry regions since the late 1980s is clearly manifested in all data sets. The main results can be summarized as follows:

1. Significant development of dry regions has been observed in Western, Central, and Eastern Europe since the late 1980s.
2. From the late 1980s to the present, the extent of the dry regions has increased by approximately 7%.
3. There was a slight decrease in the dry-wet transition and a slight increase in the wet-dry transition from 1950 to 2019.
4. Throughout the study period, Northern Europe and the UK were classified as wet regions, while the Iberian Peninsula and the southern tip of the Balkan Peninsula as dry regions.
5. The development of dry areas was mainly found in France, Germany, Poland, Czechia, the Pannonian Basin, and the region between Belarus and Ukraine.

The results demonstrate the long-term development of dry regions since the late 1980s, mainly in Western and Central Europe in all data sets, and in Eastern Europe in CRU and E-OBS. Compared to CRU and E-OBS, ERA5 has low values of aridity index mainly in Eastern Europe, due to the overestimation of precipitation, and should be interpreted with caution.

Acknowledgements We acknowledge E-OBS from the EU-FP6 project UERRA, the Copernicus Climate Change Service and Climate Data Store, and the data providers in the ECA&D project, the Climatic Research Unit, and ECMWF.

Author contribution ZB, PM, JK: conceptualization, review, and editing. ZB: writing—original draft, data processing, visualization. FS: visualization review and editing. MV, US, YM, MH: review and editing.

Funding The study was supported by the Czech Science Foundation, project 20-28560S (“Driving mechanisms of extremes in reanalysis and climate models”). ZB was also supported within student project “Conditional probabilities of transition from arid to humid

environment and vice versa in Europe during the period 1766–2015” by the Internal Grant Agency of the Faculty of Environmental Sciences.

Data availability The data sets generated and analyzed during the current study are available from the corresponding author on reasonable request.

Code availability Not applicable.

Declarations

Ethics approval The authors have agreed for authorship, read and approved the manuscript, and given consent for submission and subsequent publication of the manuscript.

Consent to participate All authors consent to participate in the present study.

Consent for publication All authors read the manuscript and agree for the publication.

Conflict of interest The authors declare no competing interests.

References

- Allan R, Pereira L, Smith M (1998) Crop evapotranspiration (guidelines for computing crop water requirements). FAO Irrigation and drainage paper 56. Food and Agriculture Organization
- Arora VK (2002) The use of the aridity index to assess climate change effect on annual runoff. *J Hydrol* 265(1):164–177
- Ault TR (2020) On the essentials of drought in a changing climate. *Science* 368(6488, SI):256–260
- Bandhauer M, Isotta F, Lakatos M, Lussana C, Baserud L, Izsak B, Szentes O, Tveito OE, Frei C (2022) Evaluation of daily precipitation analyses in E-OBS (v19.0e) and ERA5 by comparison to regional high-resolution datasets in European regions. *Int J Climatol* 42(2):727–747
- Barrow CJ (1992) World Atlas of Desertification (United Nations Environment Programme). *Land Degradation & Development* 3(4):249
- Bautista F, Bautista D, Delgado-Carranza C (2009) Calibration of the equations of Hargreaves and Thornthwaite to estimate the potential evapotranspiration in semi-arid and subhumid tropical climates for regional applications. *Atmosfera* 22(4):331–348
- Bell B, Hersbach H, Berrisford P, Dahlgren P, Horányi A, Muñoz Sabater J, Nicolas J, Radu R, Schepers D, Simmons A, Soci C, Thépaut JN (2020) ERA5 monthly averaged data on single levels from 1950 to 1978 (preliminary version). Copernicus Climate Change Service (C3S) Climate Data Store (CDS)
- Birsan MV, Dumitrescu A (2014) ROCADA: Romanian daily gridded climatic dataset (1961–2013) V1.0
- Blöschl G, Sivapalan M, Wagener T, Viglione A, Savenije H (2013) Runoff prediction in ungauged basins (synthesis across processes, places and scales). Cambridge University Press, United Kingdom
- Budyko MI (1974) *Climate and Life*. Academic Press, London
- Carmona AM, Poveda G, Sivapalan M, Vallejo-Bernal SM, Bustamante E (2016) A scaling approach to Budyko’s framework and the complementary relationship of evapotranspiration in humid environments: case study of the Amazon River basin. *Hydrol Earth Syst Sci* 20(2):589–603

- Chang X, Wang S, Gao Z, Luo Y, Chen H (2019) Forecast of daily reference evapotranspiration using a modified daily Thornthwaite Equation and temperature forecasts. *Irrig Drain* 68(2):297–317
- Cheval S, Dumitrescu A, Birsan M-V (2017) Variability of the aridity in the South-Eastern Europe over 1961–2050. *Catena* 151:74–86
- Cornes RC, van der Schrier G, van den Besselaar EJM, Jones PD (2018) An ensemble version of the E-OBS temperature and precipitation data sets. *J Gerontol Ser A Biol Med Sci* 123(17):9391–9409
- Creed IF, Spargo AT, Jones JA, Buttle JM, Adams MB, Beall FD, Booth EG, Campbell JL, Clow D, Elder K, Green MB, Grimm NB, Miniati C, Ramlal P, Saha A, Sebestyen S, Spittlehouse D, Sterling S, Williams MW, Winkler R, Yao H (2014) Changing forest water yields in response to climate warming: results from long-term experimental watershed sites across North America. *Global Change Biol* 20(10):3191–3208
- Dai A (2011) Drought under global warming: a review. *WIREs Clim Change* 2(1):45–65
- Diaz-Padilla G, Sanchez-Cohen I, Guajardo-Panes RA, Del Angel-Perez AL, Ruiz-Corral A, Medina-Garcia G, Ibarra-Castillo D (2011) Mapping of the aridity index and its population distribution in Mexico. *Revista CHapingo Serire Ciencias Forestales y Del Ambiente* 17(SI):267–275
- Duan Z, Chen Q, Chen C, Liu J, Gao H, Song X, Wei M (2019) Spatiotemporal analysis of nonlinear trends in precipitation over Germany during 1951–2013 from multiple observation-based gridded products. *Int J Climatol* 39(4):2120–2135
- Fibbi L, Chiesi M, Moriondo M, Bindi M, Chirici G, Papale D, Gozzini B, Maselli F (2016) Correction of a 1 km daily rainfall dataset for modelling forest ecosystem processes in Italy. *Meteorol Applications* 23:294–303
- Gao X, Giorgi F (2008) Increased aridity in the Mediterranean region under greenhouse gas forcing estimated from high resolution simulations with a regional climate model. *Global Planet Change* 62(3–4):195–209
- Gardelin M, Lindstrom G (1997) Priestley-Taylor evapotranspiration in HBV-simulations. *Nordic Hydrol* 28(4–5):233–246
- Gerrits AMJ, Savenije HHG, Veling EJM, Pfister L (2009) Analytical derivation of the Budyko curve based on rainfall characteristics and a simple evaporation model. *Water Resour Res* 45(4):W04403, 1–15
- Hanel M, Rakovec O, Markonis Y, Maca P, Samaniego L, Kysely J, Kumar R (2018) Revisiting the recent European droughts from a long-term perspective. *Sci Rep* 8:9499, 1–11
- Hargreaves G, Samani Z (1985) Reference crop evapotranspiration from temperature. *Appl Eng Agric* 1(2):1–12
- Harris I, Jones PD, Osborn TJ, Lister DH (2014) Updated high-resolution grids of monthly climatic observations - the CRU TS3.10 Dataset. *Int J Climatol* 34(3):623–642
- Harris I, Osborn TJ, Jones P, Lister D (2020) Version 4 of the CRU TS monthly high-resolution gridded multivariate climate dataset. *Scient Data* 7(1):109, 1–18
- Hassler B, Lauer A (2021) Comparison of reanalysis and observational precipitation datasets including ERA5 and WFDE5. *Atmosphere* 12(11):1462, 1–30
- Herrera S, Gutiérrez JM, Ancell R, Pons MR, Frías MD, Fernández J (2012) Development and analysis of a 50-year high-resolution daily gridded precipitation dataset over Spain (Spain02). *Int J Climatol* 32(1):74–85
- Hersbach H, Bell B, Berrisford P, Biavati G, Horányi A, Muñoz Sabater J, Nicolas J, Peubey C, Radu R, Rozum I, Schepers D, Simmons A, Soci C, Dee D, Thépaut JN (2018) ERA5 monthly averaged data on single levels from 1959 to present, Copernicus Climate Change Service (C3S) Climate Data Store (CDS). <https://doi.org/10.24381/cds.fl7050d7>
- Hijmans RJ (2021) raster: Geographic data analysis and modeling. R package version 3.5-2. <https://CRAN.R-project.org/package=raster>
- Hofstra N, Haylock M, New M, Jones PD (2009) Testing E-OBS European high-resolution gridded data set of daily precipitation and surface temperature. *J Gerontol Ser A Biol Med Sci* 114:D21101, 1–16
- Huang J, Ji M, Xie Y, Wang S, He Y, Ran J (2016) Global semi-arid climate change over last 60 years. *Clim Dyn* 46(3–4):1131–1150
- Huguenin MF, Fischer EM, Kotlarski S, Scherrer SC, Schwierz C, Knutti R (2020) Lack of change in the projected frequency and persistence of atmospheric circulation types over Central Europe. *Geophys Res Lett* 47(9):e2019GL086132, 1–10
- Isotta FA, Vogel R, Frei C (2015) Evaluation of European regional reanalyses and downscalings for precipitation in the Alpine region. *Meteorologische Zeitschrift* 24(1):15–37
- Keyantash JA, Dracup JA (2004) An aggregate drought index: assessing drought severity based on fluctuations in the hydrologic cycle and surface water storage. *Water Resour Res* 40(9):W09304, 1–13
- Kohli G, Lee CM, Fisher JB, Halverson G, Variano E, Jin Y, Carney D, Wilder BA, Kinoshita AM (2020) ECOSTRESS and CIMIS: A comparison of potential and reference evapotranspiration in riverside county, California. *Remote Sensing* 12(24):4126, 1–12
- Kucerova M, Beck C, Philipp A, Huth R (2017) Trends in frequency and persistence of atmospheric circulation types over Europe derived from a multitude of classifications. *Int J Climatol* 37(5):2502–2521
- Laiti L, Mallucci S, Piccolroaz S, Bellin A, Zardi D, Fiori A, Nikulin G, Majone B (2018) Testing the hydrological coherence of high-resolution gridded precipitation and temperature data sets. *Water Resour Res* 54(3):1999–2016
- Lakatos M, Weidinger T, Hoffmann L, Bihari Z, Horvath A (2020) Computation of daily Penman-Monteith reference evapotranspiration in the Carpathian Region and comparison with Thornthwaite estimates. *Adv Sci Res* 16:251–259
- Lang D, Zheng J, Shi J, Liao F, Ma X, Wang W, Chen X, Zhang M (2017) A comparative study of potential evapotranspiration estimation by eight methods with FAO Penman-Monteith method in southwestern China. *Water* 9(10):734, 1–18
- Lhotka O, Trnka M, Kysely J, Markonis Y, Balek J, Mozny M (2020) Atmospheric circulation as a factor contributing to increasing drought severity in Central Europe. *J Gerontol Ser A Biol Med Sci* 125(18):e2019JD032269, 1–17
- Lioubimtseva E, Cole R, Adams JM, Kapustin G (2005) Impacts of climate and land-cover changes in arid lands of central Asia. *J Arid Environ* 62(2):285–308
- Liu J, Xu S, Han X, Chen X, He R (2019) A multi-dimensional hydro-climatic similarity and classification framework based on Budyko theory for continental-scale applications in China. *Water* 11(2):319, 1–26
- Markonis Y, Kumar R, Hanel M, Rakovec O, Maca P, AghaKouchak A (2021) The rise of compound warm-season droughts in Europe. *Sci Adv* 7(6):eabb9668, 1–7
- Moravec V, Markonis Y, Rakovec O, Svoboda M, Trnka M, Kumar R, Hanel M (2021) Europe under multi-year droughts: how severe was the 2014/2018 drought period? *Environ Res Lett* 16(3):034062, 1–13
- Myronidis D, Nikolaos T (2021) Changes in climatic patterns and tourism and their concomitant effect on drinking water transfers into the region of South Aegean, Greece. *Stoch Env Res Risk Assess* 35:1725–1739
- Naumann G, Cammalleri C, Mentaschi L, Feyen L (2021) Increased economic drought impacts in Europe with anthropogenic warming. *Nat Clim Chang* 11(6):485–491

- Navarro A, Garcia-Ortega E, Merino A, Luis Sanchez J, Kummerow C, Tapiador FJ (2019) Assessment of IMERG precipitation estimates over Europe. *Remote Sens* 11(21):2470, 1–17
- Nechita C, Cufar K, Macovei I, Popa I, Badea ON (2019) Testing three climate datasets for dendroclimatological studies of oaks in the South Carpathians. *Sci Total Environ* 694:133730, 1–10
- Nyman P, Sherwin CB, Langhans C, Lane PNJ, Sheridan GJ (2014) Downscaling regional climate data to calculate the radiative index of dryness in complex terrain. *Aust Meteorol Oceanographic J* 64(2):109–122
- Oudin L, Hervieu F, Michel C, Perrin C, Andreassian V, Anctil F, Loumagne C (2005) Which potential evapotranspiration input for a lumped rainfall-runoff model? Part 2 Towards a simple and efficient potential evapotranspiration model for rainfall-runoff modelling. *J Hydrol* 303(1-4):290–306
- Paltineanu C, Mihailescu IF, Secseanu I, Dragota C, Vasenciu F (2007) Using aridity indices to describe some climate and soil features in Eastern Europe: a Romanian case study. *Theoret Appl Climatol* 90(3-4):263–274
- Pan N, Wang S, Liu Y, Li Y, Xue F, Wei F, Yu H, Fu B (2021) Rapid increase of potential evapotranspiration weakens the effect of precipitation on aridity in global drylands. *J Arid Environ* 186:104414, 1–9
- Peng L, Li Y, Feng H (2017) The best alternative for estimating reference crop evapotranspiration in different sub-regions of mainland China. *Scient Reports* 7:5458, 1–19
- Pereira AR, Pruitt WO (2004) Adaptation of the Thornthwaite scheme for estimating daily reference evapotranspiration. *Agricultural Water Management* 66(3):251–257
- Poyen FB, Ghosh AK, Kundu P (2016) Review on different evapotranspiration empirical equations. *Int J Adv Eng Manag Sci* 2:17–24
- Pravalié R, Bandoc G (2015) Aridity variability in the last five decades in the Dobrogea Region, Romania. *Arid Land Res Manag* 29(3):265–287
- R Core Team (2021) R: a language and environment for statistical computing. R Foundation for Statistical Computing, Vienna, Austria. <https://www.R-project.org/>
- Rakovec O, Samaniego L, Hari V, Markonis Y, Moravec V, Thober S, Hanel M, Kumar R (2022) The 2018–2020 multi-year drought sets a new benchmark in Europe. *Earths Future* 10(3):e2021EF002394, 1–11
- Rehor J, Brazdil R, Trnka M, Lhotka O, Balek J, Mozny M, Stepanek P, Zahradnick P, Mikulova K, Turna M (2021) Soil drought and circulation types in a longitudinal transect over central Europe. *Int J Climatol* 41(1):E2834–E2850
- Rolle M, Tamea S, Claps P (2021) ERA5-based global assessment of irrigation requirement and validation. *Plos One* 16(4):e0250979, 1–21
- Salvati L, Sateriano A, Zitti M (2013) Long-term land cover changes and climate variations—a country-scale approach for a new policy target. *Land Use Policy* 30:401–407
- Samani Z (2000) Estimating solar radiation and evapotranspiration using minimum climatological data. *J Irrig Drain Eng* 126(4):265–267
- Sanchez E, Romera R, Gaertner MA, Gallardo C, Castro M (2009) A weighting proposal for an ensemble of regional climate models over Europe driven by 1961–2000 ERA40 based on monthly precipitation probability density functions. *Atmos Sci Lett* 10(4):241–248
- Sarbu I, Sebarchievici C (2017) Solar heating and cooling systems (fundamentals, experiments and applications). Academic Press, London
- Seiller G, Anctil F (2016) How do potential evapotranspiration formulas influence hydrological projections? *Hydrol Sci J* 61(12):2249–2266
- Sentelhas PC, Gillespie TJ, Santos EA (2010) Evaluation of FAO Penman-Monteith and alternative methods for estimating reference evapotranspiration with missing data in Southern Ontario, Canada. *Agri Water Manag* 97(5):635–644
- Sfica L, Beck C, Nita A-I, Voiculescu M, Birsan M-V, Philipp A (2021) Cloud cover changes driven by atmospheric circulation in Europe during the last decades. *International Journal of Climatology* 41(1):E2211–E2230
- Skok G, Zagar N, Honzak L, Zabkar R, Rakovec J, Ceglar A (2016) Precipitation intercomparison of a set of satellite- and raingauge-derived datasets, ERA Interim reanalysis, and a single WRF regional climate simulation over Europe and the North Atlantic. *Theoretical and Applied Climatology* 123(1-2):217–232
- Spinoni J, Vogt J, Naumann G, Carrao H, Barbosa P (2015) Towards identifying areas at climatological risk of desertification using the Koppen-Geiger classification and FAO aridity index. *Intern J Climatol* 35(9):2210–2222
- Tabari H (2010) Evaluation of reference crop evapotranspiration equations in various climates. *Water Resour Manage* 24(10):2311–2337
- Tapiador FJ, Sanchez E (2008) Changes in the European precipitation climatologies as derived by an ensemble of regional models. *J Climate* 21(11):2540–2557
- Tegos A, Malamos N, Koutsoyiannis D (2015) A parsimonious regional parametric evapotranspiration model based on a simplification of the Penman-Monteith formula. *J Hydrol* 524:708–717
- Tomczyk AM, Bednorz E, Polrolniczak M (2019) The occurrence of heat waves in Europe and their circulation conditions. *Geografie* 124(1):1–17
- van der Schrier G, van den Besselaar EJM, Tank AMGK, Verver G (2013) Monitoring European average temperature based on the E-OBS gridded data set. *J Gerontol Ser A Biol Med Sci* 118(11):5120–5135
- Van Loon AF (2015) Hydrological drought explained. *Wiley Interdisciplinary Reviews-Water* 2(4):359–392
- Velikou K, Lazoglou G, Tolika K, Anagnostopoulou C (2022) Reliability of the ERA5 in replicating mean and extreme temperatures across Europe. *Water* 14(4):543, 1–15
- Wald L (2018) Basics in solar radiation at Earth surface. <https://www.researchgate.net/publication/322314967>
- Wang D, Alimohammadi N (2012) Responses of annual runoff, evaporation, and storage change to climate variability at the watershed scale. *Water Resour Res* 48(5):W05546, 1–16
- Weiland FCS, Tisseuil C, Durr HH, Vrac M, van Beek LPH (2012) Selecting the optimal method to calculate daily global reference potential evaporation from CFSR reanalysis data for application in a hydrological model study. *Hydrol Earth Syst Sci* 16(3):983–1000
- Wickham H (2016) ggplot2: Elegant graphics for data analysis. Springer-Verlag New York. <https://ggplot2.tidyverse.org>
- Wilhite DA (2000) Droughts: a global assessment, Chapter 1: Drought as a Natural Hazard: Concepts and Definitions. Routledge, London
- Winter TC, Rosenberry DO, Sturrock AM (1995) Evaluation of 11 equations for determining evapotranspiration for a small lake in the North Central United-States. *Water Resour Res* 31(4):983–993
- Xiang K, Li Y, Horton R, Feng H (2020) Similarity and difference of potential evapotranspiration and reference crop evapotranspiration - a review. *Agri Water Manag* 232:106043, 1–16

- Xu CY, Singh VP (2000) Evaluation and generalization of radiation-based methods for calculating evaporation. *Hydrol Process* 14(2):339–349
- Xu J, Peng S, Ding J, Wei Q, Yu Y (2013) Evaluation and calibration of simple methods for daily reference evapotranspiration estimation in humid East China. *Archives of Agronomy and Soil Science* 59(6):845–858
- Zhao H, Pan X, Wang Z, Jiang S, Liang L, Wang X, Wang X (2019) What were the changing trends of the seasonal and annual aridity indexes in northwestern China during 1961–2015? *Atmospheric Res* 222:154–162
- Zheng H, Zhang L, Zhu R, Liu C, Sato Y, Fukushima Y (2009) Responses of streamflow to climate and land surface change in the headwaters of the Yellow River Basin. *Water Res Res* 45(7):W00A19, 1–9
- Zhou S, Yu B, Huang Y, Wang G (2015) The complementary relationship and generation of the Budyko functions. *Geophys Res Lett* 42(6):1781–1790
- Zveryaev II, Gulev SK (2009) Seasonality in secular changes and interannual variability of European air temperature during the twentieth century. *J Geophys Res-Atm* 114:D02110, 1–14
- Zveryaev II (2004) Seasonality in precipitation variability over Europe. *J Gerontol Ser A Biol Med Sci* 109(D5):D05103, 1–16

Publisher's note Springer Nature remains neutral with regard to jurisdictional claims in published maps and institutional affiliations.

Springer Nature or its licensor (e.g. a society or other partner) holds exclusive rights to this article under a publishing agreement with the author(s) or other rightsholder(s); author self-archiving of the accepted manuscript version of this article is solely governed by the terms of such publishing agreement and applicable law.